WEMPEC

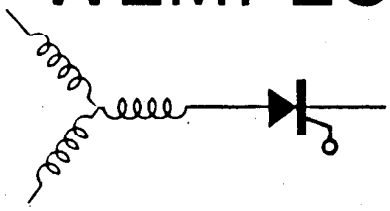

Wisconsin Electric Machines and Power Electronics Consortium

RESEARCH REPORT
82-2

A Quantitative Analysis of Induction Motor Performance Improvement by SCR Voltage Control

T.M. Rowan
University of Wisconsin
Madison, Wisconsin

T.A. Lipo
University of Wisconsin
Madison, Wisconsin

Department of Electrical and Computer Engineering
University of Wisconsin-Madison
Madison, Wisconsin 53706

April 1982

A Quantitative Analysis of Induction Motor Performance Improvement by SCR Voltage Control

TIMOTHY M. ROWAN AND THOMAS A. LIPO, SENIOR MEMBER, IEEE

Abstract—**Minimum input power and maximum efficiency operation occur at characteristic slip values which can be realized for any induction motor operating at part load by properly adjusting the amplitude of the applied stator terminal voltages. These two criteria are shown to yield perceptibly different results when the motor is driven from a silicon-controlled rectifier (SCR) voltage controller. In addition, it is demonstrated that a constant power factor controller results in an operating regime which is substantially poorer than operation at either minimum input power or maximum efficiency. It is further shown that minimum stator current and minimum power factor angle criteria yield results which are closer to the ideal than the constant power factor controller.**

INTRODUCTION

VARIABLE voltage operation of a squirrel cage induction machine at part load is receiving considerable attention as an energy conservation measure. In particular, the power factor controller introduced by Nola [1], [2] has created an interest in energy-saving schemes for all types of electric motors. Subsequent papers [3], [4] have suggested the potential of the power factor controller for energy saving, particularly in industrial and commercial applications which include substantial periods at light load. While three-phase and single-phase motors employing both fixed frequency and variable frequency supplies can exploit voltage control, this paper will be concerned primarily with fixed frequency three-phase drives.

Although energy savings is claimed by all manufacturers of such devices, the amount of savings that can actually be realized has apparently never been quantified in the literature. This omission can probably be attributed primarily to the difficulty in calculating such data. However, since the cost of such a voltage controller is several times the cost of the installed motor, a need clearly exists to demonstrate that its payoff period will justify the purchase of such a device.

Thus far, the available theory devoted to this concept is based on ideal sinusoidal excitation [5]. It is well-known, however, that thyristor voltage control results in considerable harmonic distortion due to the use of phase back thyristors to interrupt the flow of stator current. The goal of this paper is to quantify the efficiency improvements that can be realized with practical voltage controllers and to compare these results to the ideal sine wave case. In particular, the effects of practical system behavior will be investigated which specifically include the effects of the magnetizing inductance, the core loss, the stray no-load loss, the harmonics caused by the phase back, and the silicon-controlled rectifier (SCR) conduction loss nonlinearities.

Optimal values of the thyristor delay angle will be calculated and compared to the results obtained using a conventional constant power factor control scheme. The potential of possible alternative control schemes will be discussed. Duty cycle curves will be presented for a specific machine. These duty cycle curves are restricted to the motor studied. However, they are representative of the type of curves which would enable the application engineer to attain a reasonable understanding of the potential energy savings that can be realized for a specific application. The approach suggested in this paper is sufficiently general that the same technique can be applied to many motor drive applications.

BASIC CONCEPT

Simply stated, efficiency improvement by voltage control is achieved by reducing the applied voltage whenever the torque requirement of the load can be met with less than full motor flux. The reduced motor flux results in reduced core loss and also in reduced stator copper loss, since the magnetizing component of stator current is reduced. The reduced air gap flux, however, also requires a larger slip to produce the required torque compared to operation at full rated flux. Hence the slip dependent rotor loss and load component of the stator copper loss are increased. By proper adjustment of these two loss components the fundamental component losses can be minimized for most part-load operating conditions. Harmonic losses in the motor as well as thyristor losses are introduced, however, so that the net energy savings is decreased. These additional losses could, in fact, outweigh the savings gained by reducing the fundamental loss components.

The nature of the efficiency improvement attainable can be illustrated by considering an idealized situation wherein the motor parameter variations are neglected and the voltage controller is assumed to be modeled by an ideal adjustable amplitude sine wave source in series with a resistance. Under these assumptions the equivalent circuit of Fig. 1 applies. As is well-known, conventional constant voltage operation of an induction machine results in a motor slip which varies in proportion to the required load torque. In general, the load torque is considered as the independent variable and the slip, power factor, input power, efficiency, etc., are considered as the dependent variables. Clearly, from Fig. 1, the only variable quantity in the circuit is the slip, and hence the input impedance, power factor, input power, and efficiency may be con-

Paper IPCSD 82-63, approved by the Industrial Drives Committee of the IEEE Industry Applications Society for presentation at the 1982 IEEE Power Electronics Specialists Conference, Cambridge, MA, June 14-17. Manuscript released for publication December 21, 1982.

The authors are with the Department of Electrical and Computer Engineering, University of Wisconsin-Madison, 1425 Johnson Drive, Madison, WI 53706.

0093-9994/83/0700-0545$01.00 © 1983 IEEE

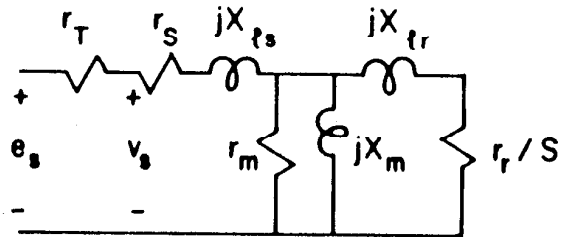

Fig. 1. Conventional per phase equivalent circuit including SCR losses.

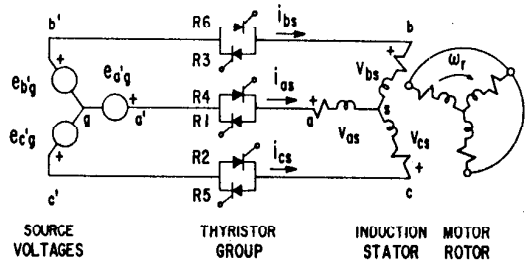

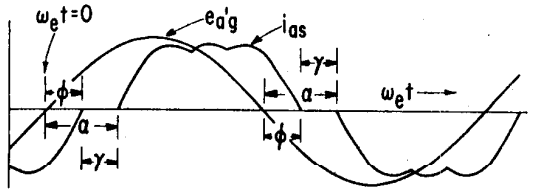

Fig. 2. Induction motor voltage controller employing inverse parallel connected SCR's and resulting waveforms.

sidered as functions of slip. For fixed input voltage, load changes are accomodated by changes in the slip S. When slip varies, so do the power factor, current, input power, and efficiency. If, as an alternative, the voltage to the machine is adjusted to supply the required load while the slip is held constant, then the efficiency and power factor would remain fixed. It follows that if the optimal slip frequency can be located and the power factor held constant at its corresponding value, then this optimal value of motor efficiency could be maintained over a range of partload conditions. Regrettably, however, the nonlinearities in the motor and SCR characteristics prevent this ideal value from being attained.

PRINCIPLES OF PHASE BACK VOLTAGE CONTROL

Fig. 2 shows a schematic diagram of a practical three-phase induction motor voltage controller. In this circuit, three triacs or six inverse parallel connected SCR's are placed in series with the motor supply. Voltage control is implemented by delaying the conduction of the oncoming thyristors with respect to their natural forward conduction point and hence interrupting the flow of current in the motor lines. Although the motor phase voltages are progressively reduced as the delay in the firing point of the SCR's increases, the voltages also become increasingly distorted. The harmonics contained in the motor voltage waveform produce harmonic currents which result in additional losses which are not present in a simple sine wave control. In addition, the SCR's themselves produce losses which are most severe when the devices are phased fully on.

Fig. 2 also illustrates typical voltage and current waveforms observed during operation of the circuit. In this figure the angle γ which expresses the time in degrees during which the current is zero is called the hold-off angle. The angle corresponding to the instant at which the oncoming SCR is triggered with respect to the voltage zero crossing is generally called the delay angle α. The angle ϕ is somewhat erroneously called the power factor angle and is the angle between the voltage zero intersection and the corresponding current zero intersection. This angle is equal to the true power factor angle when the SCR phase delay is zero but does not have the same physical significance when phase delay is occurring. The power factor angle ϕ is maintained constant in the Nola power factor controller.

Solution of the circuit of Fig. 2 involves the analysis of a mixed boundary condition problem in which the voltages across each of the three stator windings are defined for a portion of a cycle, while the winding currents are specified as zero for the remainder of the cycle. The solution of this problem can be accomplished by the use of the orthogonal axis theory in which the symmetry of the three-phase system is utilized to solve for those boundary conditions which yield a valid steady-state solution to the system differential equations. The theory used to define and solve this problem is given in detail in [6] and will not be discussed further in this paper. However, comparison with test data indicates that such solutions can be obtained with only marginal error and therefore warrant application to the optimization problem described in this paper. A typical computed solution taken from [6] is shown in Fig. 3 together with the corresponding experimental results.

The motor selected for this study has undergone a series of careful measurements in order to establish the proper machine parameters [5]. The benchmark motor is a 7 1/2-hp three-phase Baldor machine. The measured magnetizing reactance X_m and combined core loss and stray no-load loss resistance r_m are shown as per unit quantities in Fig. 4 as a function of air gap line-to-line voltage. The remaining parameters in per unit are shown in Table I. Negligible deep bar effect was observed with this machine, so that the rotor parameters are assumed constant and not frequency dependent. Because voltage variation affects the flux level in the machine, the core loss resistance and magnetizing reactance become functions of air gap voltage. The characteristic for r_m has been adjusted to include the effects of stray no-load losses which are also a function of air gap voltage. These losses result from rotor currents flowing in the machine due to slotting.

Although the curve of X_m versus voltage is typical, the curve for r_m is somewhat unexpected, since the measurements indicate a peaking in this quantity near 80 percent voltage. However, the decrease in r_m for large values of voltage has been observed in the past [7] and is probably caused by the increased eddy currents resulting from the flux wave tending to become flat-topped at higher saturation levels. The stray load losses which occur due to the flow of load current has been neglected primarily because a simple model for this effect is lacking. The contribution of stray load losses is only a

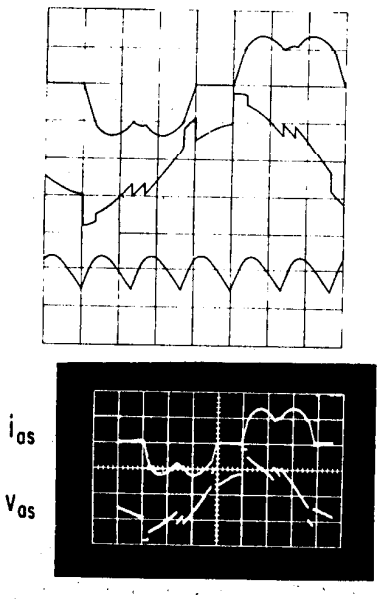

Fig. 3. Typical calculated voltage and current waveforms and corresponding experimental results. $\gamma = 45°$, phase current $i_{as} = 1.0$ A/div, phase voltage $v_{as} = 100$ V/div, torque = 0.5 Nm/div.

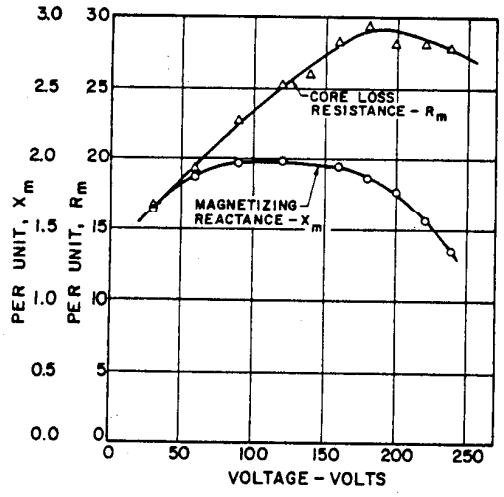

Fig. 4. Magnetizing reactance X_m and core loss resistance r_m as function of air gap line-to-line voltage.

TABLE I
NAMEPLATE DATA AND PER UNIT PARAMETERS OF TEST MACHINE

Nameplate Data	Baldor Electric Co. 7.5 HP, Frame 924M 284T 208/230/440 Volts 21/20/10 Amps
Per Unit Parameters	
	$r_s = 0.023$ $X_{ls} = 0.0962$
	$r_r = 0.014$ $X_{lr} = 0.0962$
	r_m, X_m - See Fig. 4

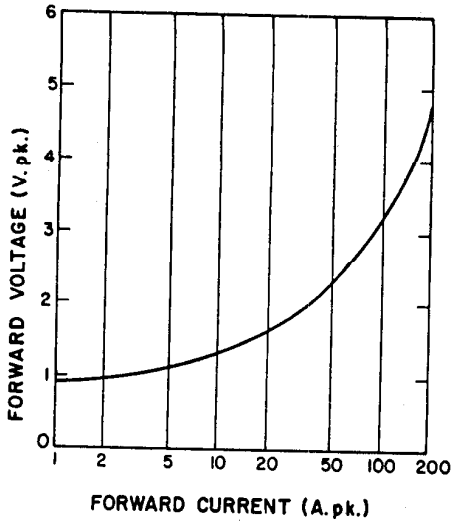

Fig. 5. Forward voltage drop of T400-16 SCR.

small fraction of the total losses and will be assumed to have negligible effect on the results of this paper. The final component of losses, friction, and windage also has been neglected. These losses are of nonelectrical origin and are essentially constant since the variation in rotor speed with load is negligible. Hence they can be considered simply as part of the load torque.

The laboratory thyristor voltage controller used during the experiment phase of this study was a 50-hp model. Since per unit losses would not be typical, it was decided to substitute the *V-I* characteristics with an SCR controller more appropriate for the 7 1/2-hp motor rating. For this purpose a Westinghouse Series T400-16 phase control SCR was selected. The forward voltage drop of this device as a function of forward current is shown in Fig. 5.

One feature of the solution method outlined in [6] is that a noniterative closed-form solution of the motor currents is obtained. However, this previous work did not account for SCR drops, core loss, or saturation effects. The nonlinearities imposed by saturation combined with the SCR nonlinearity unfortunately prevent a closed-form solution, and iteration must now be introduced. In this paper a simple Newton-Raphson scheme was used to converge on a solution. Convergence was not a problem and was typically achieved within four or five iterations. The solution thereby obtained was then used to iterate on the parameter of interest at a particular load point of interest (for example, maximum efficiency at a specified load). This complexity, however, introduced two additional levels of iteration which added substantially to the computation time. As a result, approximately six hours of main frame computer time was involved throughout the course of this study.

PERFORMANCE CHARACTERISTICS

Fig. 6 shows the torque speed characteristics of the 7 1/2-hp Baldor machine as a function of the hold-off angle γ. Superimposed on these curves are located trajectories of maximum efficiency η and minimum input power P_{in} for a range of constant load torques from 1.0 to 0.0. Note that both of

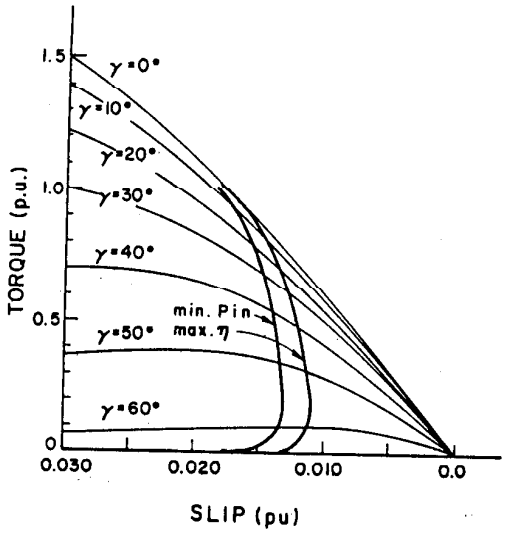

Fig. 6. Torque-slip characteristics of 7 $\frac{1}{2}$-hp Baldor machine as function of hold-off angle showing loci of maximum efficiency and minimum input power.

these curves follow the $\gamma = 0$ curve (SCR's fully on) until the load torque is less than a certain critical value beyond which phase control commences. The minimum power dashed curve occurs at a lower speed than for maximum efficiency. The curves are not identical, since motor losses are minimized in the case of maximum efficiency, while input power includes the effect of changes in output power as well as motor losses.

In Fig. 7 the corresponding motor efficiency as a function of the motor torque is plotted. In particular, the dot-dash curve represents the efficiency that can be realized when the motor is fed from a constant amplitude, sinusoidal supply at rated voltage. The efficiency peaks at 92.0 percent but thereafter falls precipitously as load is reduced. It should be mentioned that this efficiency value is perhaps two percentage points better than those usually encountered in a machine of this rating [8]. Since a voltage controller is better suited to reduce the losses of a motor of poor efficiency, the results that will be obtained in this paper can be expected to be somewhat pessimistic.

If the power factor at the maximum efficiency point ($T = 0.9$) is selected for control and is held fixed for torques below this value, the dashed curve of Fig. 7 is obtained. In this case the voltage supply is again assumed to be an ideal zero impedance adjustable amplitude sine wave supply. Although a constant parameter analysis indicates that the motor will operate at constant efficiency, it is interesting to note that the efficiency actually increases somewhat, peaking at about 92.2 percent with a load torque of 0.55 pu. This behavior is due to the peaking in the core loss resistance r_m and magnetizing reactance X_m of Fig. 4.

The two curves discussed thus far assume that the supply voltage is ideal. When this ideal sine wave supply is replaced by a practical SCR controller the maximum efficiency condition can again be located with the aid of a digital computer. The solid curve of Fig. 7 illustrates the results obtained after iterating for the best achievable efficiency at each load condition. This curve corresponds to the maximum efficiency

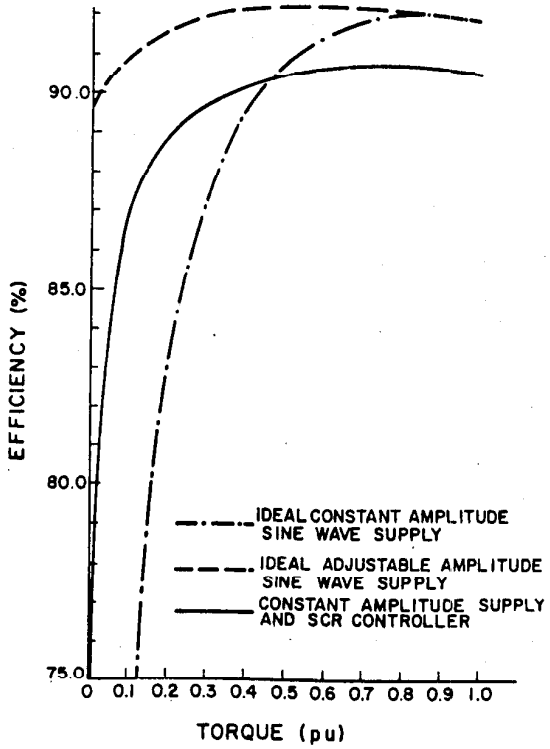

Fig. 7. Efficiency of Baldor machine as function of load torque for three types of ideal supplies.

locus sketched on Fig. 6. A substantial drop in efficiency over the entire load range is immediately apparent.

Since phase back commences only below values of load less than 0.9 pu, harmonics do not appear in the supply line above this point. Hence the efficiency decline at full load (1.0 pu) can be attributed entirely to the forward conduction drop in the inverse-parallel connected SCR's. The subsequent deviation of the two curves below 0.9 load results from the losses introduced by the harmonic currents in the motor lines which can become appreciable at light loads. Note that the solid and dot-dashed curves cross at a load of approximately 0.45 pu which suggests that a net increase in power loss will result if the motor is operated from the SCR controller at loads above 0.45 pu. It is immediately evident that the motor must be operated at light loads for substantial periods of time if any savings at all are to be realized. The intersection of these two curves will always occur for any system, but the intersection point will clearly change from motor to motor. This intersection point could be utilized as a criterion to determine whether the use of a voltage controller would result in a net energy saving.

Thus far, the efficiency curve defined by the solid curve corresponds to the best possible efficiency that can be obtained with a given SCR controller. In practice, this curve can be considered as an unattainable ideal, since continuous operation along this curve would imply optimization of efficiency either by feedback control or by open loop programming of the SCR firing angle. Either approach is clearly a formidable task and appears to be impractical at the present time.

The solid curve of Fig. 7 showing the best efficiency η for a

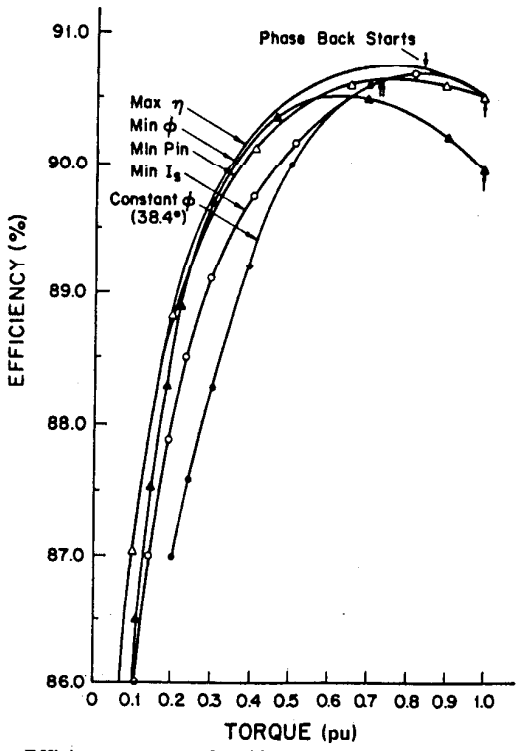

Fig. 8. Efficiency curves of Baldor machine comparing four types of practical control schemes to ideal maximum efficiency characteristic.

practical SCR controller is reproduced in Fig. 8. This curve can be used as a reference to examine various types of practical control schemes. In particular, four control algorithms are shown corresponding to constant power factor angle, minimum stator current, minimum power factor angle, and minimum stator power.

Perhaps, the most widely used method of control is described in the original patent of Nola [1] and is commonly called the Nola power factor controller. This method, identified as the curve with solid dots in Fig. 8, derives its name from the fact that the power factor angle ϕ is regulated to a constant value. Note that the efficiency realized by this method suffers substantially when compared to the ideal case. While not explicitly shown, this curve crosses the constant sinusoidal voltage curve at only 0.36 pu torque which suggests that a savings in energy with a conventional Nola controller will be difficult to attain, at least with the motor studied, unless the motor is very lightly loaded for a substantial period of time. In practice, other difficulties also occur.

In principle, the most practical value of power factor angle to regulate again appears to be the power factor angle for maximum sine wave efficiency similar to that used for the dashed curve of Fig. 7. This point occurs at the 0.9 pu load condition with the case of constant amplitude sine wave supply shown in Fig. 7. Unfortunately, it can be shown that this particular value of ϕ, 38.4°, cannot be realized for any value of firing angle α during light load conditions. That is, the range of all possible values of ϕ for loads less than 0.2 is always greater than 38.4°. In order to realize operation at smaller loads, set point values of ϕ greater than 38.4° must be chosen. Unfortunately, as a result, the part-load and full-load efficiencies begin to decline seriously. In order to reach operation at no load, a power factor angle of 45.2° must be selected. However, the efficiencies at part-load needed to maintain this angle become so poor that the corresponding efficiencies cannot be located on Fig. 8. This inherent limitation in the Nola controller has apparently been recognized by its inventor [9].

Fig. 8 shows the performance of three potential control algorithms which could be used to avoid the problems encountered by the conventional Nola controller. The first, corresponding to the open dot curve of Fig. 8, shows the efficiency that results when the stator current amplitude is minimized [10]. This curve is again substantially far from the optimum. However, the problem of reaching feasible operating points at both light and heavy loads has been avoided.

The second proposed method, the solid triangle curve, indicates the variation in efficiency obtained when the angle ϕ in Fig. 3 is minimized for each load condition rather than regulated constant. Note that this characteristic is much closer to the optimum curve except at high values of torque, where it deviates rapidly from the optimum. This behavior suggests that practical use of this algorithm requires that it be switched out of the circuit above some predetermined maximum and the SCR's simply set for maximum conduction.

The open triangle curve of Fig. 8 is a proposed method which shows how the efficiency changes when the input power is minimized. This curve corresponds to the second of the heavy solid lines in Fig. 6. Note that, while resulting in an efficiency somewhat less than the ideal, the degradation is relatively small over the entire operating range, about 0.3 percent maximum. In contrast to efficiency, the power input could be easily measured and potentially used as a control variable for the purposes of optimization.

In Fig. 9 are plotted the hold-off angle γ, the delay angle α, and the power factor angle ϕ for the optimum efficiency case (solid line curve of Figs. 7 and 8). Note that ϕ is not constant, as is the case for the power factor controller, but varies by as much as 10°. This curve clearly indicates why maintaining maximum efficiency is difficult when ϕ is held constant.

Although efficiency calculations indicate the effectiveness of the energy conversion, they do not provide a measure of the amount of energy actually saved. Fig. 10 is a curve of actual watts saved as a function of load torque for the ideal case and for a number of the practical control schemes. The dashed curve again corresponds to the case in which the motor is supplied with ideal adjustable amplitude sine waves. Note that, ideally, power savings could be realized over the entire range of load torque. The solid curve again indicates the situation in which the ideal voltage controller is replaced by a practical SCR controller with ideal control. A substantial drop in power savings is indicated, and in fact, a "negative savings" is obtained for load conditions above 0.5 pu. The possibility of actual savings is clearly dependent on the amount of time spent at no-load or light-load conditions.

The most satisfactory overall control algorithm is the minimum power control indicated again by open triangles on Fig. 10. Note that in this case the curve is actually located slightly

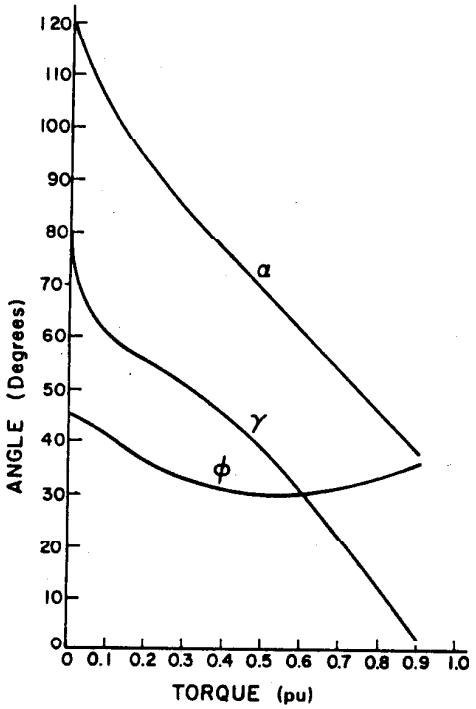

Fig. 9. Hold-off angle γ, power factor angle ϕ, and delay angle α for optimum efficiency case with practical SCR voltage controller.

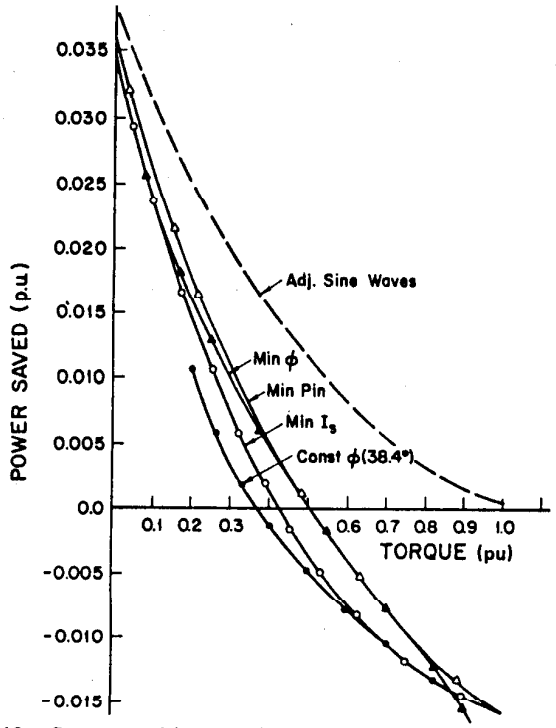

Fig. 10. Power saved in per unit as function of per unit load torque for ideal sine wave controller and SCR controller with four practical control algorithms.

above the ideal control since power input has, in fact, been minimized. The next best control algorithm is the minimum ϕ controller again indicated by solid triangles. The minimum stator current amplitude and constant ϕ controllers are also shown. These results again indicate substantial degradation in performance, particularly at part load. In particular, a net loss in energy savings with the constant power factor controller is indicated for all load conditions greater than 0.35 pu.

APPLICATION CONSIDERATIONS

In many applications a motor is subjected to two distinct load conditions. First, a heavy-load condition occurs in which the motor is performing useful work. The object of this operating mode is clearly to perform the work as quickly and efficiently as possible. In this case, maximum efficiency is of primary concern. This operating condition, however, occurs at a sufficiently large value of load, typically 1.0 pu that the voltage controller need only be phased fully on. The second condition corresponds to a light-load condition in which the load has essentially been removed. Since no useful work is being done, the objective during this mode is not necessarily to operate the motor at its peak efficiency. Clearly, energy saving is now of primary concern so that a criterion centered on minimizing the input power rather than maximizing the efficiency is of importance. Hence a minimum power controller offers other potential advantages in addition to its feasibility as a control variable.

Fig. 11 shows a duty cycle curve in which the load is assumed to vary between two load torque conditions, full-load or 1 pu and a fraction of rated load ranging from 0.1 to 0.9 pu. The curve gives the watts saved as a function of the "duty cycle" for the case where the input power is minimized. The duty cycle is defined to be the percent of the time spent at the heavy-load condition. Note that for part load above 0.5 pu no savings at all can be obtained. For a part load of 0.3 pu, the break-even point is a 33 percent duty cycle. Energy savings does not become appreciable until the part load approaches the order of 0.2 pu or less.

For purposes of comparison, Fig. 12 illustrates a similar curve using the minimum power factor control algorithm. In this case operation at part loads greater than 0.5 pu will not save energy. In order to obtain similar savings as for the minimum power controller, part loads must be on the order of 0.15 or less.

Similar curves can also be constructed for the constant power factor control algorithm, as in Fig. 13. In this case, energy savings is negligible since the part loads below 0.2 pu cannot be reached. Poor results are also obtained for other (larger) values of ϕ, and although smaller values of part load become possible, the losses at higher loads increase, making the overall result similar.

Apparently, the potential benefits of a minimum power or power factor angle controllers are sufficiently encouraging to warrant further investigation. The problem of seeking a minimum, however, is considerably more difficult than simply regulating a variable to a constant as is done for the constant power factor controller. These types of controls, involve important auxiliary considerations that thus far have been

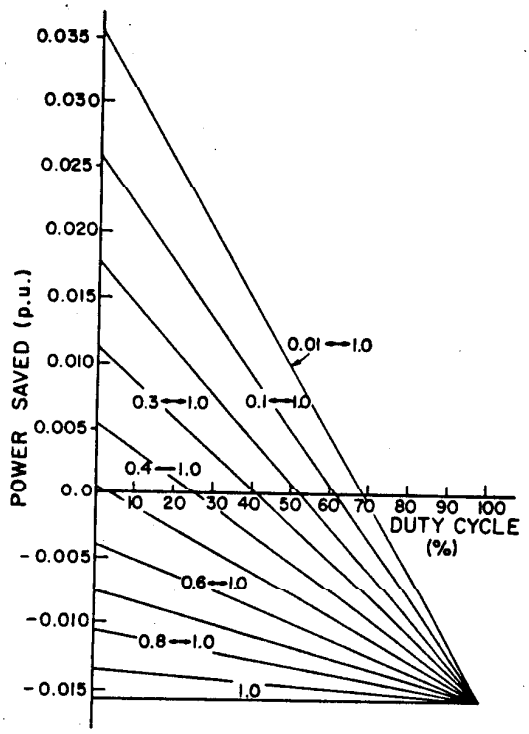

Fig. 11. Power saved versus duty cycle utilizing minimum input power control algorithm.

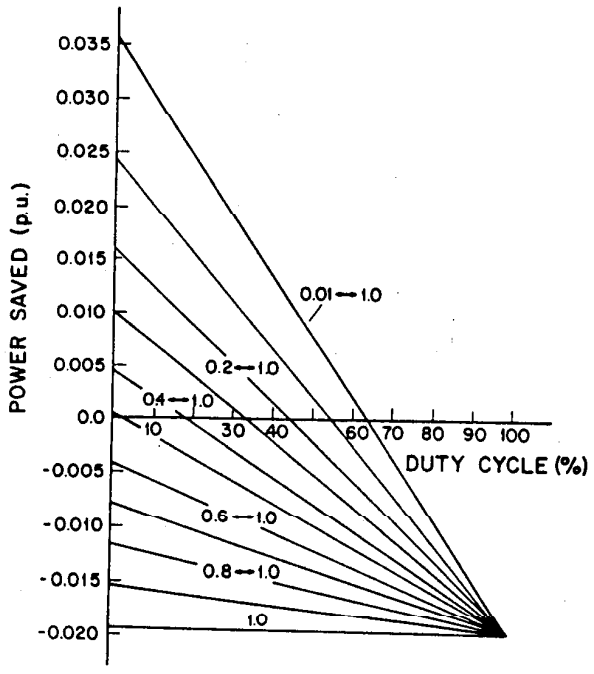

Fig. 12. Power saved versus duty cycle using minimum power factor control algorithm.

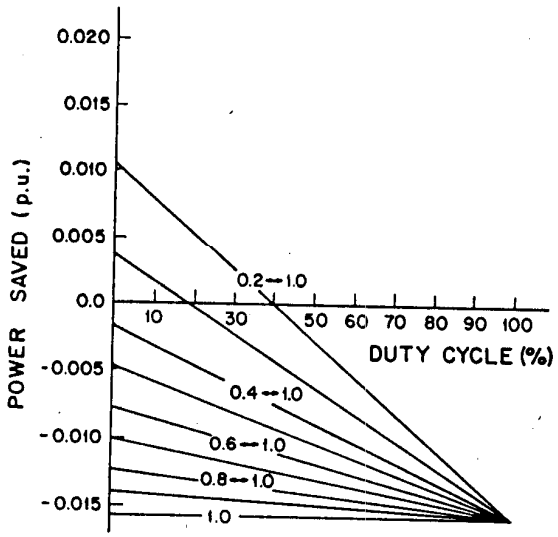

Fig. 13. Power saved versus duty cycle using constant power factor controller. Power factor angle ϕ is maintained at 38.4°.

avoided. Recall that we have been concerned only with load torque profiles which are constant, that is, independent of speed. In some applications, however, the load changes as a function of speed. For example, in fan drives the load torque variation is essentially a function of speed squared. In this case the minimum power point will not exist at finite speed but will occur at the stalled condition. In effect, this control algorithm then decides that the minimum power input will be obtained when the power output is zero. Although this will certainly be the case, the result is clearly not satisfactory. In order to overcome this problem, the user must specify how much speed reduction he is willing to tolerate during the light-load condition. However, a significant reduction in speed could affect the overall response of the motor drive since the motor must be called upon to accelerate rapidly from its unloaded speed condition as the load is applied. Hence the issue of transient response comes into play, which is outside the scope of this paper. Although the issues are complex, the benefits of such controls certainly warrant their further investigation.

APPLICATION OPPORTUNITIES

Since the curves presented in the previous sections suggest only a marginal benefit from SCR voltage control, it might be questioned whether opportunities exist in which voltage control is clearly beneficial. Such a situation frequently occurs when, due to overconservatism, erroneous information, or misapplication, the motor selected is oversized for its application. In such situations the motor is operated continuously at a load condition far removed from its maximum efficiency point. Although the motor appears to be inefficient, the problem is actually due to the fact that the fixed excitation losses are relatively high when compared to the work being done. This difficulty can be corrected by essentially reducing the excitation losses to bring them in line with the load power demand.

This problem can be simulated with the 7 1/2-hp Baldor machine if the full-load condition is assumed to occur at some

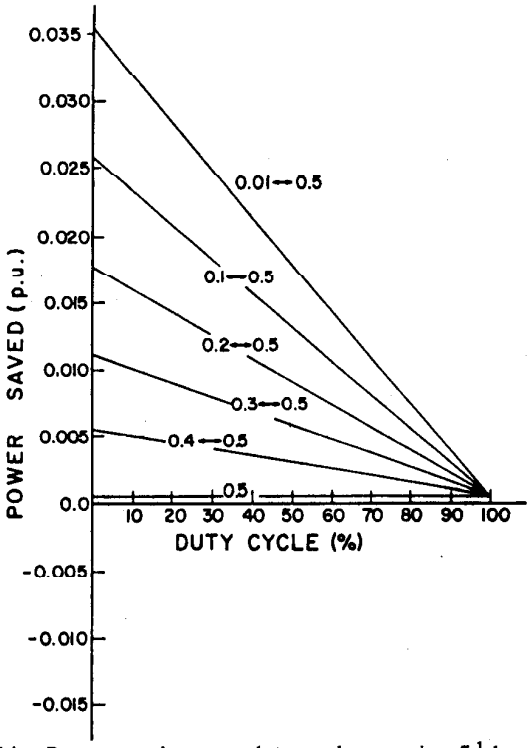

Fig. 14. Power saved versus duty cycle assuming $7\frac{1}{2}$-hp Baldor machine is oversized by 100 percent.

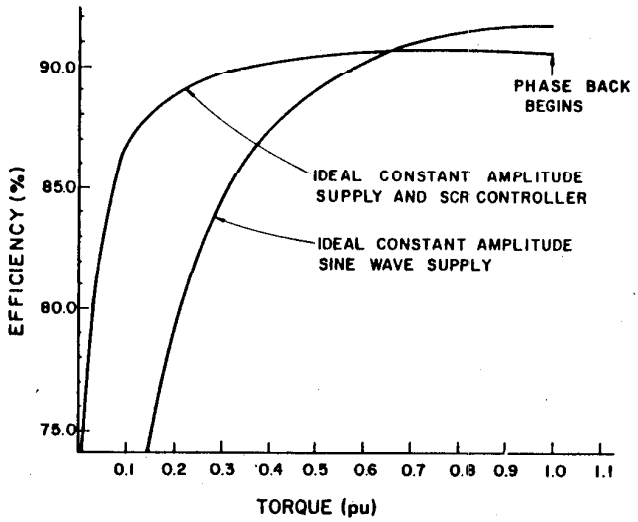

Fig. 15. Efficiency as function of load torque when motor operates with ten-percent overvoltage.

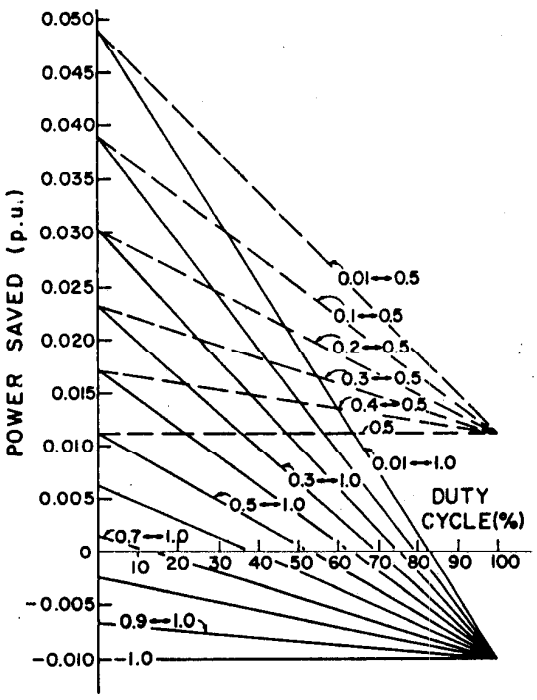

Fig. 16. Duty cycle curves of Baldor machine operating with ten-percent overvoltage, solid lines: 1.0 p.u. nominal load; dashed lines: 0.5 p.u. nominal load.

part load, for example, 0.5 pu rather than at 1.0 pu load. Duty cycle curves similar to Fig. 11 can again be constructed for this case as shown in Fig. 14. Note that, in contrast to Fig. 11, the duty cycle curves are now almost entirely in the upper half-quadrant, making the energy savings positive for any part load. Although these results appear encouraging, this situation is in actuality an expensive remedy to a misapplied motor. Clearly, a better decision to make in such a case might be simply to retrofit with a new (less expensive) motor properly rated for load demand.

A second reoccurring problem occurs when motors are located in environments in which the terminal voltages are continually at or near the overvoltage limit specified by National Electric Manufacturing Association (NEMA). This situation frequently occurs when the motor is located at the beginning of long feeder lines or in the evening hours on capacitor compensated lines, during which time the entire system is lightly loaded. In this mode the motor operates with increased excitation losses. Efficiency therefore decreases, since a corresponding increase in output does not occur.

Fig. 15 shows a modified efficiency versus load torque curve for the 7 1/2-hp Baldor machine when the terminal voltage is increased by ten percent (253 V). Note that the intersection of the maximum efficiency curve with the efficiency for constant voltage curve occurs at 0.6 pu rather than 0.45 as in Fig. 6. Fig. 16 shows another set of duty cycle curves for this case. Examination of these curves clearly shows that the opportunity for power saving is considerably enhanced. Although the previous situation clearly has better solutions, alternative approaches to an overvoltage problem, for example, a conventional magnetic type of voltage regulator or autotransformer, are also expensive. In such cases SCR voltage controllers equipped with any of the control algorithms discussed could provide the best solution to a motor which is also subjected to duty cycle operation.

CONCLUSION

Part-load efficiency improvement of induction motors by controlling stator voltage has been examined quantitatively. The analysis has included many practical considerations such as motor and SCR nonlinearities. The results of this paper indi-

cate that energy savings will be difficult with such devices unless the motor is operated essentially unloaded for significant periods of time. Although easy to implement, the constant power factor controller does not result in an optimally controlled motor, and algorithms which minimize power factor angle or stator power appear to have substantial benefits over the constant power factor controller.

ACKNOWLEDGMENT

The authors wish to thank Mrs. Tan-Wei Jian for tests made on the 7 1/2-hp experimental machine and for assistance in interpreting test results. The authors are also indebted to Mr. Dennis Braun of Cutler-Hammer Products, Eaton Corp., Milwaukee, WI, for helpful discussions concerning the constant and minimum power factor angle controllers.

REFERENCES

[1] F. J. Nola, "Power factor control system for ac induction motor," U.S. Patent 4 052 648, Oct. 4, 1977.
[2] *Save Power in AC Induction Motors*, NASA Tech. Brief MFS-23280, Summer 1977.
[3] F. Nola, "Power factor controller—An energy saver," in *Proc. IEEE IAS Annu. Meeting*, 1980, pp. 194–198.
[4] N. Mohan, "Evaluation and comparison of state of the art techniques for energy conservation by reduced losses in ac motors," EPRI Rep. EM-2037, Sept. 1981.
[5] T. W. Jain, N. L. Schmitz, and D. W. Novotny, "Characteristic induction motor slip values for variable voltage part load performance optimization," presented at the IEEE Power Engineering Soc. Winter Meeting, Jan. 31–Feb. 3, 1982, Paper 82 WM 229-3.
[6] T. A. Lipo, "The analysis of induction motor voltage control by symmetrically triggered thyristors," *IEEE Trans. Power App. Syst.*, vol. PAS-90, pp. 515–525, Mar./Apr. 1971.
[7] C. Veinott, *Theory and Design of Small Induction Motors*. New York: McGraw-Hill, 1959.
[8] A. D. Little, Inc., "Energy efficiency and electric motors," Final Rep. Federal Energy Administration, Contract CO-04-50217-00, May 1976.
[9] *Improved Power Factor Controller*, NASA Tech. Briefs MFS-25323, Summer 1980.
[10] K. E. Opal, C. R. Kelly, and C. W. Newcamp, "Apparatus for motor current minimization," U.S. Patent 3 723 840, Mar. 27, 1973.

Timothy M. Rowan was born in Milwaukee, WI, on April 7, 1958. He received the B.S.E.E. degree with honors from Marquette University, Milwaukee, WI, in 1980, and the M.S.E.E. degree from the University of Wisconsin, Madison, in 1982, where he is presently working toward the Ph.D. degree in electrical engineering.

From 1979 to 1980 he participated in the cooperative education program at RTE Corporation, Waukesha, WI. He has been a Teaching Assistant and Research Assistant at the University of Wisconsin since 1981.

Mr. Rowan is a member of Eta Kappa Nu and Tau Beta Pi.

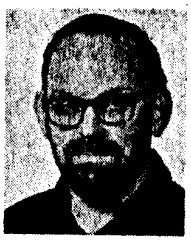

Thomas A. Lipo (M'64–SM'71) received the B.E.E. and M.S.E.E. degrees from Marquette University, Milwaukee, WI, in 1962 and 1964, respectively, and the Ph.D. degree in electrical engineering from the University of Wisconsin in 1968. He was an NRC postdoctoral fellow at the University of Manchester Institute of Science and Technology, Manchester, England, during 1968–1969.

From 1969 to 1979 he was an Electrical Engineer in the Power Electronics Laboratory of Corporate Research and Development of the General Electric Company, Schenectady, NY. While at General Electric, he pioneered the computer simulation of many types of converter systems including cycloconverters, pulsewidth modulation voltage inverters, current-source ASCI inverters, third harmonic commutated CSI inverters, and load commutated converters. He was also heavily engaged in the development of algorithms for control of solid-state converter drives for which he received several IEEE Prize Paper Awards and has received five patents with one additional pending. He has published over 50 technical papers, contributing to the analysis and design of a wide range of industrial applications including ac drives for ball mills, pumped hydro, excavators, as well as traction drives for transit cars, locomotives, and off-highway vehicles. He is currently a Professor in the Department of Electrical and Computer Engineering, University of Wisconsin-Madison.

Dr. Lipo serves on the IAS Industrial Drives Committee, the IES Drives Committee and the PES Synchronous Machine Subcommittee, Electric Machine Theory Subcommittee, and Induction Machine Subcommittee of which he is now Chairman. He has also served on the Program Committee for the IEEE Power Electronics Specialists Conference for the past six years and was Program Chairman in 1979. He is a member of the Steering Committee for the International Conference on Electrical Machines and an Associate Editor of the journal *Electric Machines and Power Systems*. He is a member of Pi Mu Epsilon, Eta Kappa Nu, Tau Betta Pi, and Sigma Xi.